Revista Mexicana de Astronomía y Astrofísica, **51**, 39–48 (2015)

INTERACTION BETWEEN THE IGM AND A DWARF GALAXY

V. Lora,[1] A. C. Raga,[2] and E. K. Grebel[1]

Received July 15 2014; accepted November 6 2014

RESUMEN

Las galaxias enanas son el tipo de objeto más común en el Universo y se cree que contienen grandes cantidades de materia oscura. Existen principalmente tres tipos morfológicos de galaxias enanas: elípticas enanas, esferoidales enanas, e irregulares enanas. Las galaxias irregulares enanas son particularmente interesantes en la evolución de galaxias enanas, ya que los predecesores de las galaxias esferoidales enanas pudieron haber sido muy similares a ellas. Entonces, debería observarse un mecanismo ligado a la pérdida de gas en las galaxias irregulares, e.g. remoción por presión de ariete (*ram pressure stripping*). En este artículo estudiamos la interacción entre el medio interestelar y un medio intergaláctico en movimiento relativo. Derivamos una solución de plasmón de choque débil que corresponde al balance entre la presión postchoque a proa y la presión estratificada del medio interestelar (que suponemos sigue la estratificación de un halo de materia obscura gravitacionalmente dominante). Comparamos nuestro modelo con simulaciones numéricas previamente publicadas y con la nube de HI que rodea las galaxias irregulares enanas Ho II y Pegaso. Mostramos que este tipo de comparación provee una forma sencilla para estimar el número de Mach del flujo.

ABSTRACT

Dwarf Galaxies are the most common objects in the Universe and are believed to contain large amounts of dark matter. There are mainly three morphologic types of dwarf galaxies: dwarf ellipticals, dwarf spheroidals and dwarf irregulars. Dwarf irregular galaxies are particularly interesting in dwarf galaxy evolution, since dwarf spheroidal predecessors could have been very similar to them. Therefore, a mechanism linked to gas-loss in dwarf irregulars should be observed, i.e. ram pressure stripping. In this paper, we study the interaction between the ISM of a dwarf galaxy and a flowing IGM. We derive the weak-shock, plasmon solution corresponding to the balance between the post-bow shock pressure and the pressure of the stratified ISM (which we assume follows the fixed stratification of a gravitationally dominant dark matter halo). We compare our model with previously published numerical simulations and with the observed shape of the HI cloud around the Ho II and Pegasus dwarf irregular galaxies. We show that such a comparison provides a straightforward way for estimating the Mach number of the impinging flow.

Key Words: galaxies: dwarf — ISM: structure — methods: analytical — methods: numerical

1. INTRODUCTION

Dwarf galaxies are the most common objects in the Universe. These galaxies contain large amounts of dark matter (DM), and are best described by a cored DM mass profile (Gilmore et al. 2007; Governato et al. 2010; Adams et al. 2014). Dwarf galaxies appear in a variety of different morphological types (Grebel 2001). In galaxy groups, the most commonly occurring types are dwarf elliptical (dE), dwarf spheroidal (dSph), and dwarf irregular (dIrr) galaxies.

Particularly, the DM content of dSphs may be as high as 90% (or more) of the total mass of the dwarf, even at the center of the galaxy, which means that the dynamics in dSph galaxies are determined

[1]Astronomisches Rechen-Institut, Zentrum für Astronomie der Universität Heidelberg, Germany
[2]Instituto de Ciencias Nucleares, UNAM, México

completely by the gravitational field of the DM halo (Binney & Tremaine 2008). dSphs have the peculiarity of containing almost no gas. If a large fraction of the gas content of a galaxy is removed, the star formation will decrease or even stop, and no stars would be formed with metallicities higher than the one of the gas at the moment of its removal.

On the other hand, dIrrs are gas-rich, irregularly shaped galaxies with recent or ongoing star formation (Grebel 1999). They have low density and low surface brightness ($\mu_B \approx 23$) and H II regions that are superposed on an underlying diffuse structure of old stars with an exponential surface brightness profile (e. g. Pasetto et al. 2003).

There are some dwarf galaxies in the Local Group (LG) which present intermediate features between dIrr and dSph, suggesting that such dwarf galaxies could be in a transition state from dIrr to dSph (Grebel et al. 2003). Transition dwarf galaxies (dTr) are dominated by old populations but contain gas and show recent star formation. They are situated at distances > 250 kpc from the large spirals, and thus could be little influenced by tidal stripping.

A very good example of a transformation of a dwarf irregular into a dwarf elliptical galaxy by ram pressure stripping is the dwarf galaxy IC3418. It presents a UV-bright tail comprised of knots, head-tail, and linear stellar features. Kenney et al.(2014) reported neither Hα nor HI emission in the main body of the galaxy, but they detected $4 \times 10^7 M_\odot$ of HI from the IC3418 tail, which suggests that the HI in the main body of the galaxy is in the process of being stripped away.

If indeed dIrrs evolve to become gas-free dSphs, there should be a mechanism or mechanisms that removes the cold gas from dIrr galaxies. It has been suggested that the gas loss could be controlled by the star formation rate and intense continuous galactic winds (Lanfranchi & Matteucci 2007), energy feedback from supernovae (Fragile et al. 2003; Marcolini et al. 2006), tidal stripping (Mayer et al. 2006), and ram pressure stripping (Mori & Burket 2000; Marcolini et al. 2003; Grebel et al. 2003; Marcolini et al. 2006; Grcevich & Putman 2009).

Ram pressure stripping has been studied numerically in great detail (Roediger & Hensler 2005; Roediger & Brueggen 2006; Roediger et al. 2006; Roediger & Brueggen 2007). For example, (Roediger & Hensler 2005) performed numerical simulations of disky galaxies in constant inter-cluster-medium winds, and found that even massive galaxies can lose a large amount of the disk gas, and even be completely stripped of their gas, if they are located in the cluster's center. Moreover, in the subsonic regime, winds with small Mach numbers are more effective in getting rid of the gas, since the inclination does not play a major role for the mass loss (Roediger & Brueggen 2006), supersonic galaxies tend to develop more irregular tails (Roediger et al. 2006), and the tail density, length, and mass distribution of a disk galaxy orbiting a galaxy cluster depends on the ram pressure as well as the galaxy's orbital velocity (Roediger & Brueggen 2008).

As a last example, (Pasetto et al. 2003) carried out N-body Tree-SPH simulations in order to investigate whether a dIrr galaxy which tidally interacts with a MW-type galaxy may be reshaped into a dSph or an elliptical object. They conclude that the transformation could be achieved, under some premises, on a time scale of $\gtrsim 4$ Gyr.

An example of a dIrr galaxy is the Ho II dwarf. Ho II is a dIrr in the M81 group (Holmberg 1950). Ho II (Walter et al. 2007; Oh et al. 2011) is very similar to the Small Magellanic Cloud (SMC) (Stanimirovic et al. 1999, 2004) in absolute magnitude ($M_B \sim -16.7$ and -16.1 respectively), HI content ($M_{HI} \sim 6 \times 10^8 M_\odot$ and $\sim 4 \times 10^8 M_\odot$ respectively) and total mass ($M = 2.1 \times 10^9 M_\odot$ and $2.4 \times 10^9 M_\odot$). The neutral gas centered on Ho II shows a cometary morphology in its outer regions with compressed contours perpendicular to its direction of motion through the IGM of the M81 group, and extended, trailing tail structures on its opposite side (Bureau & Carignan 2002; Bernard et al. 2012). It has to be noted that Ho II is probably a companion of the outlying spiral NGC 2403 and its subgroup (Karachentsev et al. 2002), which does not seem to participate in the ongoing interaction of the M81 subgroup.

A second example is the dIrr galaxy Pegasus. Pegasus belongs to the LG of galaxies and it is located at a Galactocentric distance of 919 kpc (McConnachie et al. 2005). It has a total mass of $M \simeq 3.3 \times 10^8 M_\odot$, and has a large amount of DM ($\sim 70\%$) (Kniazev et al. 2009). The Pegasus dIrr also presents the characteristic signature of ram pressure stripping (Young et al. 2003; McConnachie et al. 2007). Moreover, (McConnachie et al. 2007), conclude from the ram pressure stripping in Pegasus, and its large distance from either the Milky Way or M31, that there is evidence for the existence of a LG intergalactic medium.

In this paper we present a steady plasmon[3] model for the interaction of the ISM of a dwarf galaxy with

[3]The term plasmon was first introduced by (De Young & Axford 1967), to refer to an emiting region roughly in hydrostatic equilibrium in a co-moving frame of reference.

a flowing IGM. This model is of course appropriate for galaxies with a dense enough ISM that can balance the ram pressure of the flowing IGM. Two of the best examples of such a situation are the Ho II and the Pegasus dwarf irregulars. In this paper we develop an analytical weak-shock plasmon model for a dwarf galaxy in an IGM. We compare this analytical model with numerical simulations and observations. We show that such a comparison provides a straightforward way for estimating the Mach number of the impinging IGM flow.

We derive a simple plasmon model along the lines of the model of (De Young & Axford 1967) in § 2, balancing the post-bow shock pressure with the pressure of a stratified gas cloud. Our model has two important differences with respect to the plasmon of (De Young & Axford 1967):

- the shock is not assumed to be strong,
- the gas has a radial stratification which follows the profile of a dark matter halo (which is assumed to be gravitationally dominant over the stellar component of the dwarf galaxy).

Applications of the model to the case of a $1/R^2$ ISM pressure stratification (§ 3) and to two distributions with flat cores (§ 4) are presented. These solutions are then compared in § 4 with the numerical simulations of ram-pressure stripping flows of (Close et al. 2013) and with the observed shape of the HI clouds of Ho II (Bureau & Carignan 2002), and Pegasus (Young et al. 2003).

2. THE WEAK SHOCK PLASMON MODEL

The interaction between an initially spherically stratified ISM of a dwarf galaxy and the intergalactic medium (through which the galaxy is travelling) will result in a distortion of the ISM distribution, so that it is progressively more flattened in the direction of the galaxy's motion. This distortion progresses until a final configuration is reached in which the post-bow shock pressure of the intergalactic medium is approximately equal to the local pressure of the ISM of the dwarf galaxy. Once this "local pressure balance" configuration is reached, the system will continue to evolve at a slower rate through the entrainment of galactic ISM into the post-bow shock sheath.

Following (De Young & Axford 1967), who studied the case of a decelerating gas clump (see Appendix A), we derive a "plasmon solution", assuming that the region of the extragalactic/galactic medium interaction is narrow, and neglecting the centrifugal pressure of the material flowing along the interaction sheath (see Cantó et al. 1998). The structure of the flow is shown in the schematic diagram of Figure 1.

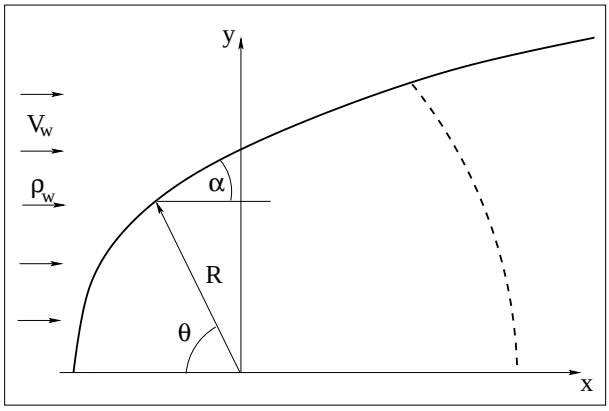

Fig. 1. In this figure we show the IGM flow in a reference frame moving with the dwarf galaxy, and with the x-axis pointing against the direction of the motion of the galaxy. The intergalactic medium impinges on the dwarf galaxy with a uniform density ρ_w and a velocity v_w, in the direction of positive x. The origin of the (x, y) coordinate system coincides with the center of the dwarf galaxy. The interaction region between IGM and the ISM of the dwarf galaxy is assumed to be thin, and is represented by the thick black curve. The θ angle is measured from the $-x$ direction, and the α angle is the angle between the locus of the interaction region and the symmetry axis.

This diagram shows the flow in a reference frame moving with the dwarf galaxy, and with the x-axis pointing against the direction of the motion of the galaxy. In this reference frame, the intergalactic medium impinges on the dwarf galaxy (with a uniform density ρ_w and a velocity v_w) in the direction of positive x. The origin of the (x, y) coordinate system coincides with the center of the galaxy, so that the unperturbed spherical pressure stratification of the galactic ISM is $P(R)$, where R is the spherical radius. The interaction region is assumed to be thin, and is represented by the thick curve (which corresponds to either the bow shock or to the outer boundary of the unperturbed galactic ISM). In the derivation of the model we use the angles θ (measured from the $-x$ direction) and α (the angle between the locus of the interaction region and the symmetry axis).

For a general (i.e., not necessarily strong) shock, the post-bow shock pressure is given by:

$$P_{PS} = \frac{2}{\gamma+1}\rho_w v_w^2 \sin^2(\alpha) - \frac{\gamma-1}{\gamma+1}P_w \ , \qquad (1)$$

where ρ_w, v_w and P_w are the density, velocity and pressure (respectively) of the impinging intergalactic medium, γ is the specific heat ratio and the angle α is shown in Figure 1. It is clear that in the weak shock limit (i.e., $v_w \rightarrow c_w = \sqrt{\gamma P_w/\rho_w}$) we correctly obtain $P_{PS} = P_w$.

Equation (1) is a straightforward generalization to the case of a general shock jump (strong or weak) of the relation used by (De Young & Axford 1967) and (Dyson 1975) to model strong (i.e., hypersonic) bow shocks.

Now, if $y(x)$ is the shape of the interaction region (see Figure 1), we have the relation:

$$\sin^2\alpha = \left[1 + \left(\frac{dx}{dy}\right)^2\right]^{-1} . \quad (2)$$

Also, the dx/dy derivative is related to the interaction surface in spherical coordinates $R(\theta)$ through:

$$\frac{dx}{dy} = \frac{\frac{-dR}{d\theta} + R\tan\theta}{\tan\theta\frac{dR}{d\theta} + R} . \quad (3)$$

Combining equations (2-3) we obtain:

$$\sin^2\alpha = \frac{\left(\tan\theta\frac{dR}{d\theta} + R\right)^2}{[(\frac{dR}{d\theta})^2 + R^2]} . \quad (4)$$

Finally, the $P_{PS} = P(R)$ condition of balance between the post-shock pressure and the spherically stratified pressure of the galactic ISM is:

$$P(R) = \frac{2}{\gamma+1}\rho_w v_w^2 \sin^2\alpha - P_w\frac{\gamma-1}{\gamma+1} , \quad (5)$$

where we have used equation (1). We then solve this equation for $\sin^2\alpha$, and combine it with equation (5) to obtain:

$$\left(\tan\theta\frac{dR}{d\theta} + R\right)^2 \cos^2\theta = F(R)\left[\left(\frac{dR}{d\theta}\right)^2 + R^2\right] , \quad (6)$$

where we have defined

$$F(R) \equiv [(\gamma+1)P(R) + P_w(\gamma+1)]\frac{1}{2\rho_w v_w^2} . \quad (7)$$

Equation (6) is a quadratic equation for $dR/d\theta$, which can straightforwardly be solved to obtain:

$$\frac{dR}{d\theta} = \frac{R}{F(R) - \sin^2\theta}\left\{\frac{\sin 2\theta}{2} - \sqrt{F(R)[1-F(R)]}\right\} . \quad (8)$$

In this way, we obtain the differential equation that describes the $R(\theta)$ shape (see Figure 1) of the interaction region between the stratified galactic ISM and the impinging intergalactic medium. We should note that the negative branch of the solution has been chosen (because this branch gives the physical solution).

One then has to integrate equation (8) with the boundary condition $R(\theta = 0) = R_0$ (the stagnation region radius), and require the shock to be perpendicular to the x-axis in the stagnation point. From equation (5), we see that this condition can be written as:

$$P(R_0) = \frac{2}{\gamma+1}\rho_w v_w - \frac{\gamma-1}{\gamma+1}P_w , \quad (9)$$

and substituting this pressure in equation (7) we obtain:

$$F(R_0) = \frac{1}{2}[2 - (\gamma-1)\frac{P_w}{\rho_w v_w^2} + \frac{(\gamma-1)}{\gamma M_w^2}] = 1 , \quad (10)$$

where $M_w = v_w/\sqrt{\gamma P_w/\rho_w}$ is the Mach number of the impinging intergalactic medium.

It is clear that equation (8) only has to be integrated until the value of θ_m for which $\sin\alpha = 1/M_w$ (see Figure 1). At this point, the shock becomes a sound wave, and detaches from the surface of the plasmon. This can be seen from the fact that if we have smaller values of α, the post-shock pressure has values $P_{PS} < P_w$ (see equation 1), so that the shock has been changed into an unphysical "expansion jump". Therefore, for $\theta > \theta_m$ the shock becomes a detached conical surface (with half-opening angle $\alpha_m = \sin^{-1}[1/M_w]$), and the surface of the plasmon is the circular surface determined from the $P(R) = P_w$ condition. This circular surface is shown with a dashed line in the schematic diagram of Figure 1.

3. THE $P(R) \propto R^{-2}$ CASE

Let us now consider the case of a galaxy with an ISM pressure stratification of the form

$$P(R) = \frac{A}{R^2} , \quad (11)$$

where A is a constant.

In terms of a dimensionless radius $r = R/R_0$ (where R_0 is the stagnation region radius), equation (8) becomes:

$$\frac{dr}{d\theta} = \frac{r}{F(r) - \sin^2\theta}\left\{\frac{\sin 2\theta}{2} - \sqrt{F(r)[1-F(r)]}\right\} , \quad (12)$$

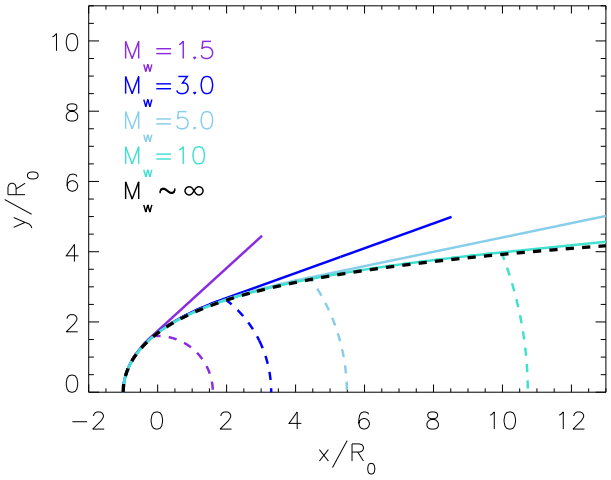

Fig. 2. In this figure we show the plasmon solutions for the values of the Mach number $M_w = 1.5, 3, 5, 10$ and ∞, of the impinging intergalactic medium (considering $\gamma = 5/3$). In this case, the dwarf galaxy has an ISM pressure stratification of the form $P(R) \propto R^{-2}$. The x-axis is pointing against the direction of the motion of the galaxy, and R_0 is the stagnation region radius.

with

$$F(r) = \frac{1}{2}\left\{\left[2 - \frac{(\gamma-1)}{\gamma}\frac{1}{M_w^2}\right]\frac{1}{r^2} + \frac{(\gamma-1)}{\gamma}\frac{1}{M_w^2}\right\}, \quad (13)$$

as obtained from equations (7), (10) and (11). As could be expected, we have not found an analytic integral for the differential equation obtained combining equations (12-13).

We therefore integrate numerically equation (12) for different values of the Mach number M_w of the impinging flow. The integration is carried out until the surface of the plasmon reaches the Mach angle $\alpha_m = \sin^{-1}(1/M_w)$ (at $\theta = \theta_m$), and for larger values of θ the shock is prolonged with the sonic slope and the plasmon is closed with a spherical surface (as described in the last paragraph of § 2). The results of this exercise are shown in Figure 2.

In this figure, we show the plasmon solutions obtained for different values of the Mach number M_w of the impinging intergalactic medium (and for an ideal monoatomic gas, i.e. $\gamma = 5/3$). In the head of the plasmons, the shock wave coincides with the surface of the plasmon, but it detaches when the normal component of the pre-shock velocity becomes sonic. Downstream of this point, the surface of the plasmon takes a constant pressure, spherical, shape, and the shock wave is a straight, sonic wave. The region of the plasmon upstream of the "sonic point" (at $\theta = \theta_m$, see above) is very similar to the solutions obtained for higher Mach number plasmons. Therefore, a good approximation to the shape of the plasmon can be obtained by taking the $M_w \to \infty$ solution of equations (12-13) and cutting it off at the value of θ_m corresponding to the actual value of M_w of the impinging intergalactic medium.

We have been unable to obtain an analytic solution of equations (12-13), even in the simple $M_w \to \infty$ case. However, it is possible to derive an approximate analytic form in the following way.

The problem that we are considering is similar to the problem of the ram pressure balance between a spherical, constant velocity wind and a uniform, streaming environment. (Dyson 1975) showed that this problem has the analytic solution $r_{Dy} = \theta/\sin\theta$ (where r_{Dy} is the spherical radius in units of the stagnation radius). We therefore propose an approximate analytic solution to our plasmon solution of the form r_{Dy}^{β}, and determine β from a fit to the $M_w \to \infty$ numerical solution of equations (12-13). In this way we obtain the approximate analytic solution:

$$r_a = \left(\frac{\theta}{\sin\theta}\right)^{1.17} \quad (14)$$

for the $M_w \to \infty$ case (which is independent of γ).

In Figure 3, we show a comparison between $r_a(\theta)$ and the $M_w \to \infty$ numerical solution, together with the associated relative error. We see that the approximate analytic solution reproduces the numerical ("exact") solution to within $\approx 2\%$, over the whole $\theta = 0 \to \pi$ range. It is then possible to obtain approximate solutions for all M_w by truncating the approximate analytic solution (equation 14) at the point at which the slope becomes sonic (with $\sin\alpha_m = 1/M_w$, see above).

Now, from the numerical solutions of equations (12-13) we compute the length-to-width ratio L/W (where L is measured along the symmetry axis from the stagnation point to the point at which the spherical back side of the plasmon intersects the axis, and the width W is twice the maximum cylindrical radius attained by the plasmon solution) as a function of the M_w Mach number (which is the only free parameter of the dimensionless plasmon solution). The results of this exercise are shown in Figure 4 (very similar results are obtained from the approximate analytic solution described above).

We see that the length-to width ratio L/W has a minimum at $M_w \approx 2$, increasing to a value of 1 (at $M_w = 1$) for smaller values of M_w, and increasing monotonically for $M_w > 2$ (see Figure 4). Actually, for $M_w < 2$ our plasmon model is probably not applicable, since for Mach numbers approaching unity

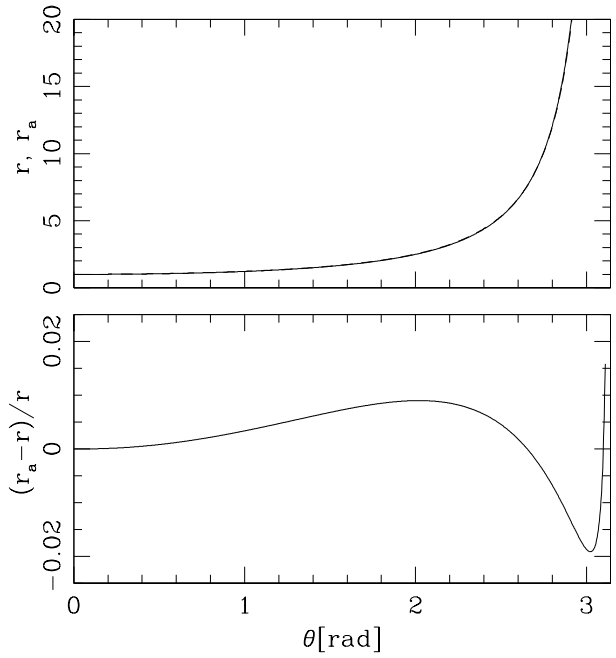

Fig. 3. In this figure, we show a comparison between the $r_a(\theta)$ approximate analytic solution (see equation 14) and the $M_w \to \infty$ "exact" numerical solution (upper panel), together with the associated relative error (bottom panel) as a function of θ (see Figure 1).

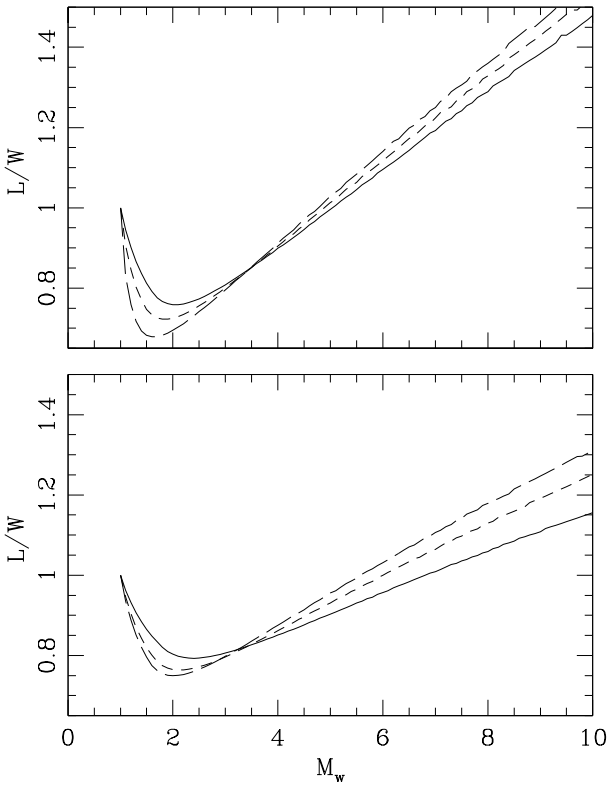

Fig. 4. In this figure we show the results of the numerical solutions of equations (12-13). We compute the length-to-width ratio L/W as a function of the Mach number M_w of the flowing IGM. We measure L along the symmetry axis, from the stagnation point to the point in which the spherical back side of the plasmon intersects the axis. The width W, is twice the maximum cylindrical radius attained by the plasmon solution. Top frame: the results obtained for the core-less pressure stratification (equation 15) are shown with the solid line, and the short-dash and long-dash lines correspond to stratifications with core radii of $R_{core} = R_0$ and $2R_0$ (respectively, see equation 15). Bottom frame: L/W as a function of Mach number for plasmons with a NFW pressure profile (see equation 19) with $R_s = 0$ (solid line) , R_0 (short dash) and $2R_0$ (long dash line).

the stand-off distance of the shock in the stagnation region becomes comparable to the radius of the plasmon, so that the "thin interaction region" approximation of our model is not valid. On the other hand, for $M_w > 2$ our plasmon model should be a reasonable approximation to the real flow.

Therefore, for a ram-pressure confined plasmon in which the impinging intergalactic medium has a Mach number $M_w > 2$, the curve shown in Figure 2 can be used to determine M_w from the length-to-width ratio of the plasmon. Of course, due to projection effects the observed length-to-width ratio is only a lower boundary of the intrinsic L/W of the plasmon, and therefore the observations only determine a lower boundary for the possible value of the Mach number M_w of the flow.

4. DISTRIBUTIONS WITH CORES

Since the dark matter component in dwarf irregular galaxies is dominant, we suppose that the gas within the dwarf galaxy follows the gravitational potential of the dark matter, therefore having the same mass density distribution. The $P(R) \propto R^{-2}$ explored in § 2 is a singular profile, but dark matter halos of dwarf galaxies are more commonly modeled either with a modified profile with a core radius (approximating the non-singular isothermal sphere solution, see, e.g., Shapiro et al. 1999) and the NFW profile (see Navarro, Frenk & White 1996).

We first explore the case of a dwarf galaxy with an ISM pressure stratification of the form:

$$P(R) = \frac{A}{(R^2 + R_{core}^2)}\,, \qquad (15)$$

with a core radius R_{core}, which is the simplest analytic approximation to the non-singular isothermal sphere (see, e.g., Hunter 2001).

Substituting this pressure stratification in equation (7) we obtain

$$F(R) = \frac{1}{2}\left[\frac{(\gamma+1)A}{\rho_w v_w^2}\frac{1}{R^2+R_{core}^2} + \frac{(\gamma-1)}{\gamma}\frac{1}{M_w^2}\right]. \quad (16)$$

Using the $F(R_0) = 1$ boundary condition (see equation 10), we have:

$$F(r) = \frac{1}{2}\left[\left(2 - \frac{(\gamma-1)}{\gamma}\frac{1}{M_w^2}\right)\left(\frac{1+r_c^2}{r^2+r_{0,c}^2}\right) + \frac{(\gamma-1)}{\gamma}\frac{1}{M_w^2}\right], \quad (17)$$

with $r = R/R_0$ and $r_c = R_{core}/R_0$, where R_0 is the stagnation region radius of the plasmon.

From numerical integrations of equations (12) and (17), we compute the length to width ratio L/W as a function of the Mach number M_w of the flow for models with core radii $R_{core} = R_0$ and $R_{core} = 2R_0$. From Figure 4, we see that the predicted values of L/W only have relatively small deviations from the values obtained for the core-less pressure distribution (see § 3).

We also compute models for a NFW mass density profile (Navarro et al. 1996) given by

$$\rho(R) = \frac{\rho_0}{\frac{r}{R_s}(1+\frac{r}{R_s})^2}\ . \quad (18)$$

Thus, the pressure of the NFW profile can be writen as:

$$P(R) = \frac{A}{R(R+R_s)^2}\ . \quad (19)$$

We compute the NFW pressure for a $R_s = 0$, R_0 and $2R_0$. The resulting L/W vs. M_w relations are shown in the bottom panel of Figure 4. From this figure we see that the length-to-width ratios only differ substantially from the L/W values obtained for the $1/R^2$ pressure law for relatively large ($M_w > 4$) Mach numbers.

From the results of this section we see that for the three studied ISM pressure distributions (equations 11, 15 and 19) we obtain a minimum value $L/W \approx 0.7 \rightarrow 0.8$ for the predicted length-to-width ratio of the plasmon shape, and that this minimum occurs for a Mach number $M_w \approx 1.7 \rightarrow 2.3$ of the impinging flow.

5. COMPARISON WITH SIMULATIONS AND OBSERVATIONS

It is possible to compare our plasmon models with the simulations of (Close et al. 2013). These authors computed 3D numerical simulations of ram-pressure stripping of a structure with a NFW profile (equation 19) for an impinging flow with Mach numbers $M_w = 0.9$, 1.1 and 1.9.

The simulations of (Close et al. 2013) produce a recognizable core and an extended, lower density wake of stripped material (see their Figure 2). The cores of the $M_w = 0.9$ and 1.1 simulations have length to width ratios $L/W \approx 1$, consistent with the $M_w \rightarrow 1$ limit of our plasmon model (see Figure 4), though our model is not clearly applicable to such low Mach numbers. The $M_w = 1.9$ simulation of (Close et al. 2013) produces a flattened core, with $L/W \approx 0.7$ (see the $t = 2512$ Myr time frame of their Figure 3). This length-to-width ratio is clearly consistent with the L/W values predicted from our plasmon model for $M_w = 2$ (see the bottom frame of Figure 4).

Let us now compare our plasmon model with the HI maps of Ho II. From the map of (Bureau & Carignan 2002), using the $N_H = 6 \times 10^{19}\mathrm{cm}^{-2}$ contour (see their Figure 3), we calculate a length-to-width ratio $L/W = 0.8 \pm 0.1$. This value is consistent with the predictions from our plasmon model for any of the pressure distributions that we have studied, for Mach numbers $M_w \approx 1.5 \rightarrow 3$ (see the two frames of Figure 4).

This comparison between the HI emission of Ho II and our model is strictly correct only if the motion of Ho II lies on the plane of the sky. In order to evaluate the possible projection effects, we take a $M_w = 2$, core-less pressure stratification (equation 11) plasmon model, and rotate its axis by an arbitrary angle ϕ with respect to the plane of the sky.

The projected length-to-width ratios computed from the rotated plasmon model as a function of ϕ are shown in Figure 5. From this figure, we see that the projected L/W value slowly increases with increasing ϕ up to an angle $\phi \approx 40°$, and then rises more rapidly to the expected $L/W = 1$ value for $\phi = 90°$ (that is, with the symmetry axis along the line of sight). From this exercise we conclude that the straightforward comparison of the L/W ratio of Ho II with the (unprojected) values predicted from our plasmon models is probably reasonable, since projection effects become important only for rela-

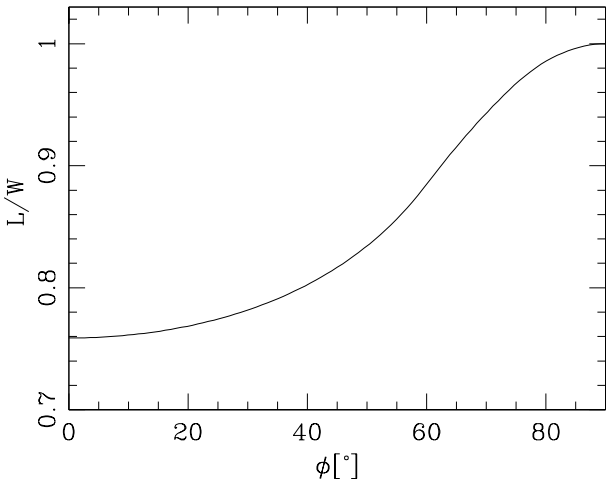

Fig. 5. Predicted L/W ratio for a core-less, inverse square pressure stratification (equation 11), $M_w = 2$ plasmon as a function of the angle ϕ between the symmetry axis and the plane of the sky.

tively large values of ϕ. Such large values of the orientation angle have low probabilities of occurrence, since they correspond to directions pointing into a small solid angle.

We now compare the plasmon model with the Pegasus dwarf HI maps of (Young et al. 2003) (see their Figure 5). We take the contours $N_H = 4 \times 10^{19}\mathrm{cm}^{-2}$ and $N_H = 1.6 \times 10^{20}\mathrm{cm}^{-2}$, and compute a very similar length-to-width ratio for both contours, $L/W = 1.5 \pm 0.1$ and $L/W = 1.4 \pm 0.1$ respectively.

If we compare this value of L/W of the Pegasus dwarf with the predictions from our plasmon model (top panel of Figure 4), we deduce a high Mach number of $M_w \approx 9$ for the LG IGM.

6. CONCLUSIONS

We describe a simple plasmon model for the interaction of a dwarf galaxy with a stratified ISM (following the stratification of a dark matter halo) and a surrounding ISM flowing at a relatively low Mach number. We use this model to compute the resulting confined shapes for different forms of the ISM pressure stratification.

From these models we have calculated the length-to-width ratios of the plasmon shapes, finding that in all cases a minimum L/W value of ≈ 0.8 is obtained for a $M_w \approx 2$ Mach number for the flowing IGM. We find that the predicted values of L/W are consistent with the aspect ratios of the central cores of the 3D numerical simulations of (Close et al. 2013). In addition, the fact that numerical simulations do produce an approximately steady, plasmon-like core (unlike the De Young & Axford's 1967 "decelerating cloud plasmon" which is not reproduced in numerical simulations) indicates that our plasmon solution is indeed applicable to real astrophysical flows.

Finally, if we look at the shape of the HI cloud surrounding the Ho II dwarf spheroidal, we find that it has a length-to-width ratio ≈ 0.8, consistent with the predicted plasmon shapes for $M_w \approx 2$. We argue that the observed shape of the Ho II cloud is unlikely to be strongly affected by projection effects, so that this is a valid comparison with our model.

For the Pegasus dIrr, we find a length-to-width ratio ≈ 1.5 which indicates a very large Mach number ($M_w \approx 9$) for the intra-cluster medium. The large value of the Mach number seems unlikely for a galaxy at the location of Pegasus. On the other hand, the LG intergalactic medium might be clumpy; therefore, it is possible that Pegasus is moving through a higher density and lower temperature region, compared to other dwarf galaxies in the LG (McConnachie et al. 2007), and as a consequence would present a larger Mach number.

Clearly, these comparisons between the plasmon and specific objects is correct only if the velocity of the galaxies with respect to the intergalactic medium lies close to the plane of the sky. In § 5, we argue that projection effects should be small (so that a direct comparison with the models without projection corrections is appropriate) for angles between the direction of motion and the plane of the sky $\phi < 40°$. Higher values of ϕ have lower probabilities of occurrence (orientation angles $\phi > 40°$ have probabilities of occurrence $p = 1 - \sin 40° = 0.36$), but, of course, could be relevant for specific objects. An important projection effect (obtained for $\phi > 40°$) would result in an underestimate of the Mach number of the flow.

We should note that an application of our plasmon model to observed galaxies is clearly only relevant if the ram-pressure stripping mechanism is actually active in the observed objects. As discussed in § 1, this is only one of the possible mechanisms for stripping the ISM from dwarf galaxies.

Our present semi-analytic model gives an approximate prediction of the shape expected for the ISM of a dwarf galaxy subject to the gravitational force of a dark matter potential and the ram pressure of an impinging intergalactic medium. This model can be used to estimate the flow parameters (in particular, the Mach number of the impinging flow) that would produce the observed shape. These results could then be fed into a numerical simulation (e.g.,

like the ones of Close et al. 2013) in order to obtain more detailed predictions of the observational characteristics of the flow (e.g., 21cm line emission maps and velocity channel maps). A comparison between such predictions and observations would be useful for showing whether or not the ram-pressure stripping mechanism is actually responsible for the observed structure of the ISM.

V.L. gratefully acknowledges support from the FRONTIER grant from the University of Heidelberg. AR acknowledges support from CONACYT grants 101356, 101975 and 167611, and DGAPA-UNAM grants IN105312 and IG100214. We also acknowledge an anonymous referee for helpful comments.

APPENDIX A
THE PLASMON OF DE YOUNG & AXFORD

(De Young & Axford 1967) derived the pressure balance plasmon shape for a decelerating gas clump. In this problem, if the plasmon is isothermal and has a constant deceleration a, its internal pressure has an exponential stratification:

$$P(x) = P_0 e^{-x/H} \,, \tag{A20}$$

where x is the distance along the symmetry axis measured from the stagnation point, $H = RT/\mu a$ (with T the temperature, R the gas constant and μ the mean molecular weight) is the pressure scale-height and P_0 is the pressure at the stagnation point. The shape of the plasmon is then derived by setting $P(x) = P_{PS}$ (the post-shock pressure). Using equations (1) and (2), this condition gives:

$$\frac{dx}{dr} = \sqrt{\frac{1}{\kappa + [1-\kappa]e^{-x/H}} - 1} \,, \tag{A21}$$

where $\kappa = 1/m_w^2$ with

$$m_w = \sqrt{\frac{2\gamma}{\gamma - 1}} M_w \,, \tag{A22}$$

where M_w is the Mach number of the streaming environment. The plasmon solution of (De Young & Axford 1967) is derived from equation (A21) with $\kappa = 0$. For non-zero κ his equation has the analytic solution:

$$\frac{r}{H} = \tan^{-1}\left(\frac{2\sqrt{1-u}\sqrt{a+u}}{2u+a-1}\right) + \sqrt{a}\,\log\left[\frac{2a+u(1-a)+2\sqrt{a}\sqrt{1-u}\sqrt{a+u}}{au}\right], \tag{A23}$$

where

$$a = \frac{1}{m_w^2 - 1} = \frac{\kappa}{1-\kappa} \,. \tag{A24}$$

It is straightforward to show that for $m_w \to \infty$ equation (A23) coincides with the plasmon solution of (De Young & Axford 1967).

REFERENCES

Adams, J. J. et al., 2014, ApJ, 789, 63
Bernard, E. J., Ferguson, A. M. N., Barker, M. K., et al. 2012, MNRAS,426, 3490
Binney, J. & Tremaine S., 2008, Galactic Dynamics: Second Edition, Princeton University Press
Bureau, M. & Carignan, C. 2002, AJ, 123, 1316
Cantó, J., Espresate, J., Raga, A. C. & D'Alessio, P., 1998, MNRAS, 296, 1041
Close, J. L., Pittard, J. M., Hartquist, T. W. & Falle, S. A. E. G. 2013, MNRAS, 436, 3021
De Young, D. S. & Axford, W. I., 1967, Nature, 216, 129
Dyson, J. E. 1975, Ap&SS, 35, 299
Fragile, P. C., Murray, S. D., Anninos, P. & Lin D. N. C., 2003, ApJ, 590, 778
Gilmore, G., Wilkinson, M., Kleyna, J., et al. 2007, NuPhS, 173, 15
Governato, F. et al. 2010, Nature, 463, 203
Grcevich, J. & Putman, M. E., 2009, ApJ, 696, 385
Grebel, E. K. 1999, in IAU Symp. 192, The Stellar Content of Local Group, ed. P. Whitelock, & R. Cannon, 17
Grebel, E. K., 2001, ApSSS, 277, 231
Grebel, E. K., Gallagher, III J. S. & Harbeck, D., 2003, AJ, 125, 1926
Holmberg, E., 1950, Lund Medd. Astron. Obs. Ser. II, 128, 1
Hunter, C. 2001, MNRAS, 328, 839
Karachentsev, I. D., et al., 2002, A&A, 383, 125
Kenney, J. D. P., et al., 2014, ApJ, 780, 119
Kniazev, A. Y., Brosch, N., Hoffman, G. L., Grebel, E. K., Zucker, D. B. & Pustilnik, A., 2009, MNRAS, 400, 205
Lanfranchi, G. A. & Matteucci, F., 2007, A&A, 468, 927
Marcolini, A., Brighenti, F. & D'Ercole, A., 2003, MNRAS, 345, 1329
Marcolini, A., D'Ercole, A., Brighenti, F. & Recchi, S., 2006, MNRAS, 371, 643
Mayer, L., Mastropietro, C., Wadsley, J., Stadel, J., & Moore, B., 2006, MNRAS, 369, 1021
McConnachie, A. W., Irwin, M. J., Ferguson, A. M. N., Ibata, R. A., Lewis, G. F., & Tanvir, N. 2005, MNRAS, 356, 979
McConnachie, A. W., Venn, K. A., Irwing, M. J., Young, L. M.& Geehan, J. J., 2007, ApJ, 671, L33
Mori M. & Burkert A., 2000, ApJ, 538, 559
Navarro, J. F., Frenk, C. S. & White, D. M. 1996, ApJ, 462, 563

Oh, S.-H., de Blok, W. J. G., Brinks, E., Walter, F. & Kennicutt, R. C., 2011, AJ, 141, 193
Pasetto, S., Chiosi, C. & Carraro, G., 2003, A&A, 405, 931
Roediger, E. & Brueggen, M., 2008, MNRAS, 388, 89
Roediger, E. & Brueggen, M., 2007, MNRAS, 380, 1399
Roediger, E., Brueggen, M. & Hoeft, M., 2006, MNRAS, 371, 609
Roediger, E. & Brueggen, M., 2006, MNRAS, 369, 567
Roediger, E. & Hensler, G., 2005, A&A, 433, 875
Shapiro, P. R., Iliev, I. T., Raga, A. C. 1999, MNRAS, 307, 203
Stanimirovic, S., Staveley-Smith, L., Dickey, J. M., Sault, R. J. & Snowden, S. L., 1999, MNRAS, 302, 417
Stanimirovic, S., Staveley-Smith, L. & Jones, P. A., 2004, ApJ, 604, 176
Walter, F. et al. 2007, ApJ, 661, 102
Young, L. M., van Zee, L., Lo, K. Y., Dohm-Palmer, R. C., & Beierle, M. E. 2003, ApJ, 592, 111

E. K. Grebel and V. Lora: Astronomisches Rechen-Institut, Zentrum für Astronomie der Universität Heidelberg, Mönchhofstr. 12-14, 69120 Heidelberg, Germany (grebel, vlora@ari.uni-heidelberg.de).
A. C. Raga: Instituto de Ciencias Nucleares, Universidad Nacional Autónoma de México, Apdo. Postal 70-543, C. P. 04510, México, D. F., México (raga@nucleares.unam.mx).